

Radar Cross-Section Reduction of an Arbitrary Object Using a Resistor-Loaded Patch

Vani Vellanki, David R. Jackson, and Daniel Onofrei

Abstract – Various methods exist for reducing the radar cross section (RCS) of an object. Using radar-absorbent materials or selective sculpting can reduce an object's RCS. Another method is active cancellation, where a source is put on the object to emit a counter-signal that interferes with and therefore partially cancels the object-scattered signal (e.g., coming from a radar signal). The study presented here uses a microstrip antenna put on the surface of an object. Microstrip antennas with a bandwidth larger than the bandwidth of the incident radar signal are useful for this purpose. To increase the bandwidth of the patch antenna, a resistor loading approach is presented here. For a wide variety of incident signals in the suggested frequency band, RCS reduction can be achieved using such an antenna. Applications include the reduction of electromagnetic interference, a topic of considerable importance in an environment of ever-increasing spectrum congestion.

1. Introduction

A complete review of the many strategies for reducing radar cross section (RCS), both passive and active, may be found in [1, 2]. Decreased RCS using metasurfaces with both passive [3–6] and active [7–9] loading are examples of recent research. In [10], the authors presented a method for absorption of X-band radar emissions using a thin layer of collisional plasma, which is then studied and experimentally confirmed for normal or oblique incidence. Active impedance surfaces such as phase-switched surfaces were used in some of the RCS reduction approaches in [11]. In [12], the authors offered an active cancellation technique against synthetic aperture radar that is performed in three phases, using frequency and delay modulation.

Due to the fact that these methods are typically narrowband, several recent works have concentrated on ensuring wideband RCS reduction using active and passive loading, such as [13], in which metasurfaces were loaded with active circuitry using varactor diodes and non-Foster circuit elements to achieve a wider bandwidth of RCS reduction using real-time tunability. In [14] it was demonstrated that this technique is effective using both simulation and experimental data. Some more examples of wideband RCS reduction have been achieved by the use of optimized pixelated metasurfaces, as reported in [15]. Metamaterial surfaces resembling checkerboards, and metamaterials that are

combined with a dielectric absorber, were presented in [16].

In the method discussed here, introduced in [17], a time-varying radar signal that is reflected from a fixed object is cancelled by radiation from a patch antenna that is placed on the object. In order to increase the bandwidth of the patch antenna [18, 19], and thus effectively counter wider-band incident signals, a resistor-loaded patch is used. Results are presented to explore its effectiveness for practical radar pulses. It is assumed that the direction of arrival for the incident signal is known, and the direction for which cancellation is desired has also been specified.

2. System Design

The proposed active RCS reduction scheme is shown in a functional block diagram in Figure 1. The system consists of a sensor, an isolator, a transmission line, a phase shifter, and an amplifier. The phase shifter is optional, as the transmission line can be used to provide all the necessary phase shift. The sensor picks up the incoming radar signal. The optional high-impedance isolator helps to avoid loading the sensor. The sensor's output signal is phase-shifted and amplified, and then used to feed the microstrip patch antenna. The phase shift (due to the transmission line and optional phase shifter) and the amplifier gain are calibrated so that the patch radiates a signal that exactly cancels the natural scattering from the object, at the center frequency of the radar signal in the specified cancellation direction.

The sensor that is implemented here is a planar structure that has narrow rectangular metal arms running in the x - and y -directions, which is printed on a substrate and connected to a vertical conducting via

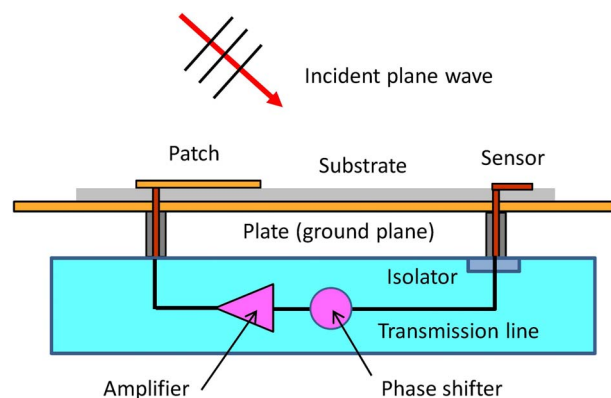


Figure 1. System diagram.

Manuscript received 28 December 2021.

Authors are with the University of Houston, Houston, TX, USA; e-mail: djackson@uh.edu.

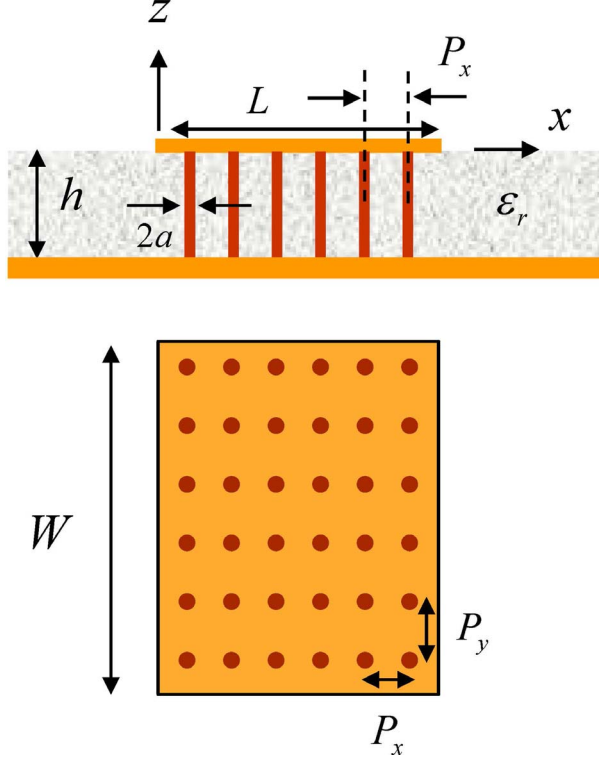


Figure 2. Side and top views of the patch with internal resistors. $L =$ resonant dimension.

that serves as the output port (only one sensor arm is shown in Figure 1). Further details are presented in [17–19]. As noted in [17–19], the success of this RCS reduction scheme depends on the patch antenna having a bandwidth that is substantially larger than the bandwidth of the incoming radar signal. Thus, having a patch with a large bandwidth is very desirable for this application to effectively reduce RCS for large-bandwidth radar signals. However, the radiation efficiency of the patch antenna is not very important in this application, since the patch only needs to radiate a small amount of power in order to effectively cancel the scattering from a distant radar transmitter. For this application it is more important that the patch have a large bandwidth and a stable TM_{10} mode of operation in order to maintain a stable pattern over the bandwidth. Hence, we propose using a resistor-loaded patch, as shown in Figure 2. A periodic arrangement of resistors within the substrate acts to artificially increase the effective loss tangent of the substrate, at the expense of radiation efficiency. In a full-wave analysis (using HFSS software), the resistors are modeled as tubes of surface impedance Z_s , giving a total impedance Z_t for each resistor, where $Z_t = Z_s(h/(2\pi a))$, where a is the radius of each tube and h is the substrate thickness, with the substrate having a relative permittivity of ϵ_r and loss tangent $\tan\delta$.

If we consider just one resistor in a unit cell, with P_x and P_y the dimensions as shown in Figure 2, then the

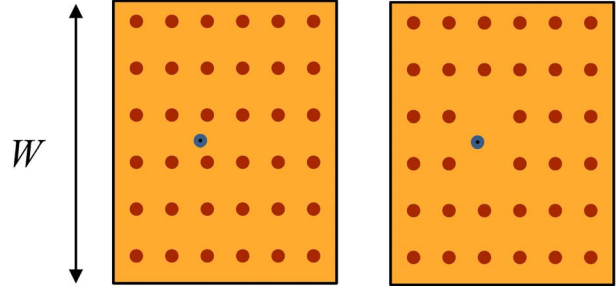


Figure 3. Patch with (left) 6×6 resistors and (right) two resistors removed. The feed is shown with a black dot. $W =$ nonresonant dimension.

effective substrate conductivity due to the resistors can be written as

$$\sigma_{\text{eff}} = \left(\frac{h}{P_x P_y} \right) \left(\frac{1}{Z_t} \right) \quad (1)$$

The effective loss tangent due to the resistors can be written as

$$\tan \delta_{\text{eff}} = \frac{\sigma_{\text{eff}}}{\omega \epsilon_0 \epsilon_r} \quad (2)$$

The total loss tangent of the patch, accounting for the internal resistors in the substrate and the natural loss tangent of the substrate, can then be written as

$$\tan \delta_{\text{tot}} = \tan \delta + \tan \delta_{\text{eff}} \quad (3)$$

In Figure 3 (at left), an array of 6×6 resistors was used. Because some of the resistors get close to the 50Ω feed point, we observed some undesired coupling with the feed. To minimize this, we removed the two resistors closest to the feed, as shown in Figure 3 (at right). This gives almost the same total loss tangent, while minimizing feed coupling.

In Table 1, designs for different patch bandwidths are shown. The rectangular patch antenna has dimensions of 6.255 cm and 10.321 cm in the x - and y -directions, respectively, with a substrate of thickness 1.524 mm and relative permittivity 2.2. The patch is designed to resonate at a frequency of 1.575 GHz (which is also the center frequency of the incident radar signal). The loss tangent of the substrate by itself is $\tan\delta = 0.001$. The resistor spacing is $P_x = 1.04$ cm and $P_y = 1.72$ cm.

Table 1. Total dielectric loss for different resistor combinations using the CAD formula and HFSS

BW	$\tan\delta_{\text{tot}}$	$\tan\delta_{\text{tot}}$ (CAD), $a = 0.083$ cm	$\tan\delta_{\text{tot}}$ (HFSS), 6×6 , $a = 0.083$ cm
2%	0.0111	0.0120	0.0124
5%	0.0536	0.0541	0.0546
10%	0.1243	0.1249	0.1253
20%	0.2658	0.2664	0.2668
50%	0.690	0.696	0.6966

Table 2. Radiation efficiency e_r (%) for different patch total loss tangents and corresponding bandwidths

$\tan\delta_{\text{tot}}$	BW (HFSS), %	e_r (CAD)	e_r (HFSS)	e_r (MWM)
0.0111	2.05	53.22	53.67	54.49
0.0536	5.10	21.11	21.45	22.26
0.1243	10.09	10.36	10.73	11.31
0.2658	20.12	5.01	5.36	5.89
0.690	50.18	2.05	2.15	2.68

The second column of Table 1 shows the necessary total loss tangent to achieve the desired bandwidth, assuming a homogeneous lossy substrate. The bandwidth is calculated using a simple computer-aided design (CAD) formula based on the substrate total loss tangent, with bandwidth = $0.7071/Q$ and $Q = 1/\tan\delta_{\text{tot}}$ [20]. The third column shows the achieved total loss tangent using the array of 6×6 resistors, based on the simple CAD formulas and using $Z_t = 29.23 \Omega$. The resistors are modeled in HFSS using a resistor tube radius of 0.083 cm. The fourth column gives the achieved total loss tangent calculated by full-wave simulation for the array of 6×6 resistors, predicted by HFSS. The agreement shows that the array of resistors can simulate well a homogenous lossy substrate with the desired loss tangent.

Table 2 shows the radiation efficiency of the same patch with a homogenous lossy substrate, for different substrate total loss tangents, along with the corresponding bandwidth and radiation efficiency. The bandwidth is now calculated using HFSS. The radiation efficiency is calculated in three different ways: a simple CAD formula for the efficiency of the patch antenna is used [20]; HFSS is used to directly calculate the efficiency; and a method that we call the “modified Wheeler method” (MWM) is used in HFSS, in which the radiation efficiency is taken as $R_{\text{in}}/R_{\text{in}0}$, where R_{in} is the input resistance at its maximum point as the frequency is swept, and $R_{\text{in}0}$ denotes the same thing for the lossless patch (no substrate or conductor loss.)

As seen from Table 2, there is good agreement in the efficiency calculations. Although the radiation efficiency becomes quite low for a large bandwidth, such as 50%, low efficiency (about 2% in this case) is still acceptable for this application. The patch thus maintains its low profile and operates in the usual TM_{10} mode while obtaining a large bandwidth.

3. Results for RCS Reduction

3.1 Scattered Signal

An analysis, as explained in [17–19], is performed for the system in Figure 1. The object is taken to be a rectangular perfect electric conducting plate of size 20 cm \times 20 cm, with the same patch antenna placed at the center of the plate. The center frequency of the incident pulse is 1.575 GHz. The patch bandwidth is 50%.

The incident signal is a rectangular chirped pulse signal that has a 2% variation in frequency across the

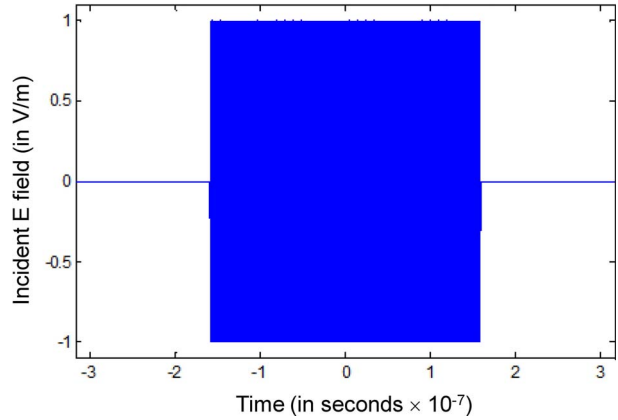


Figure 4. The incident rectangular chirped pulse signal.

width of the pulse, with a center frequency of 1.575 GHz. The frequency starts 1% lower than 1.575 GHz at the beginning of the pulse and linearly increases to 1% higher than 1.575 GHz at the end of the pulse, and the width of the rectangular chirped pulse is 317.46 ns. The incident signal is polarized with the electric field in the x -direction and is incident at normal incidence in Figure 1. This incident radar signal at the surface of the plate is shown in Figure 4. Figure 5 shows the normalized (normalized to a peak of unity) scattered signal (electric field in the x -direction) from the plate at broadside (monostatic scattering), with the scattering cancellation scheme implemented as shown in Figure 1. There is assumed to be a delay length L of one guided wavelength in the system (corresponding to the signal propagating along the transmission line) at the center frequency.

Figure 5 shows that the strongest part of the scattered signal is at the leading and trailing edges of the pulse. This is consistent with causality, as the system cannot instantaneously adjust the patch radiation to cancel changes in the incident signal, due to the delay

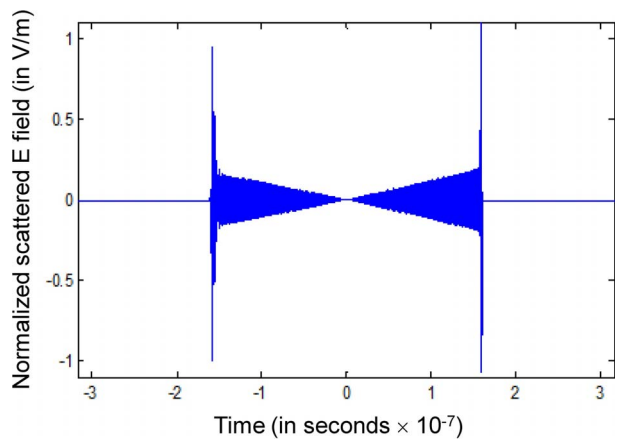


Figure 5. The rectangular chirped pulse scattered signal with scattering cancellation implemented, for a one-wavelength delay in the circuit and a patch bandwidth of 50%, using HFSS software.

Table 3. FoM (%) for case of 50% patch bandwidth with different chirp signal bandwidths, for broadside incidence and observation angle

Patch case	Chirp BW			
	2%	5%	10%	20%
50% patch BW (CAD)	0.45	0.86	2.23	15.63
50% patch BW (HFSS)	0.59	2.87	6.99	32.84
50% patch BW (HFSS, 6×6)	0.76	3.21	8.16	35.75
50% patch BW (HFSS, w/o 2)	0.65	2.94	7.08	32.98

in the system. The cancellation is best in the middle of the signal, away from the signal discontinuity, where the signal more closely resembles a pure sinusoid.

3.2 Figure of Merit

A figure of merit (FoM) is defined as the ratio of the energy in the scattered signal when the proposed RCS reduction technique is applied to the energy in the scattered signal from the same object (a $20 \text{ cm} \times 20 \text{ cm}$ plate in this study) without any RCS reduction in effect.

Table 3 shows the calculated FoM for the same rectangular chirped pulse as in Section 3.1. The FoM values for the chirped rectangular pulse are given for a 50% patch bandwidth using both a CAD method and HFSS with a homogeneous substrate (as explained in [17]), for cases with 6×6 resistors and 6×6 resistors with two resistors removed near the feed (“w/o 2”). Here there is no system delay ($L = 0$), in order to focus on the effects of the patch and signal bandwidths. The table shows that a patch with a large bandwidth (50%) can effectively reduce the RCS (achieve a low FoM) even for moderately large chirp signal bandwidths.

Table 4 shows the FoM for different patch bandwidths and chirp signal bandwidths, again with no system delay. We see that in order to get a good RCS reduction—i.e., a small FoM—the bandwidth of the patch must be significantly larger than that of the radar signal. When there is no delay in the system, the RCS reduction keeps getting smaller as the patch bandwidth increases. However, for a fixed delay in the system, results (not shown here) show that the amount of RCS reduction levels off as the patch bandwidth increases, with the lowest value of FoM achievable depending on the delay in the system. The larger the delay, the larger the smallest FoM that can be achieved. Also, for a given

Table 4. FoM (%) for different patch bandwidths and chirp bandwidths, when the incidence angle and the observation angle are both broadside, using HFSS

Patch BW	Chirp BW		
	2%	5%	10%
2%	9.49	38.41	132.49
5%	1.79	7.61	46.86
10%	0.89	4.08	12.26
20%	0.71	3.24	9.01
50%	0.68	2.98	7.14

patch bandwidth, the RCS reduction consistently gets worse as the delay in the system increases.

4. Conclusions

The scattering from an object can be reduced using the active cancellation technique presented. Effective RCS reduction for wideband signals requires a patch antenna with a large bandwidth, larger than that of the incident signal. A large-bandwidth patch that is suitable for this application is a patch with resistive loading, since a high bandwidth can be easily achieved while maintaining a low profile. The high bandwidth comes at the expense of radiation efficiency, though low efficiency can be tolerated for this low-power application.

5. References

1. E. F. Knott, J. F. Shaeffer, and M. T. Tuley, *Radar Cross Section*, Boston, Artech House, 1985.
2. P. Y. Ufimtsev, “Comments on Diffraction Principles and Limitations of RCS Reduction Techniques,” *Proceedings of the IEEE*, **84**, 12, December 1996, pp. 1830-1851.
3. J. Su, C. Kong, Z. Li, X. Yuan, and Y. Yang, “Ultra-Wideband and Polarization-Insensitive RCS Reduction of Microstrip Antenna Using Polarization Conversion Metasurface,” *Applied Computational Electromagnetics Society Journal*, **32**, 6, June 2017, pp. 524-530.
4. J. Su, C. Kong, Z. Li, H. Yin, and Y. Yang, “Wideband Diffuse Scattering and RCS Reduction of Microstrip Antenna Array Based on Coding Metasurface,” *Electronics Letters*, **53**, 16, June 2017, pp. 1088-1090.
5. L. Zhang, X. Wan, S. Liu, J. Y. Yin, Q. Zhang, et al., “Realization of Low Scattering for a High-Gain Fabry-Pérot Antenna Using Coding Metasurface,” *IEEE Transactions on Antennas and Propagation*, **65**, 7, July 2017, pp. 3374-3383.
6. Y.-J. Zheng, J. Gao, Y.-L. Zhou, X.-Y. Cao, L.-M. Xu, et al., “Metamaterial-Based Patch Antenna With Wideband RCS Reduction and Gain Enhancement Using Improved Loading Method,” *IET Microwaves, Antennas & Propagation*, **11**, 9, July 2017, pp. 1183-1189.
7. A. Kord, D. L. Sounas, and A. Alù, “Ultrathin Active Cloak With Balanced Loss and Gain,” 2016 IEEE International Symposium on Antennas and Propagation, Fajardo, PR, USA, June 26–July 1, 2016, pp. 369-370.
8. H. Li, L. Zhang, Z. Song, and X. Zeng, “RCS Reduction of Active Periodical Structural Scatterer,” 2016 11th International Symposium on Antennas, Propagation and EM Theory (ISAPE), Guilin, China, October 18–21, 2016, pp. 303-306.
9. Y. Sui, H. Gu, and C. Yang, “Reconfigurable Stealth Radome Using Active Frequency Selective Surface Technology,” 2017 IEEE International Conference on Computational Electromagnetics (ICCEM), Kumamoto, Japan, March 8–10, 2017, pp. 273-275.
10. A. Ghayekhloo, A. Abdolali, and S. H. Mohseni Armaki, “Observation of Radar Cross-Section Reduction Using Low-Pressure Plasma-Arrayed Coating Structure,” *IEEE Transactions on Antennas and Propagation*, **65**, 6, June 2017, pp. 3058-3064.
11. A. Tennant and B. Chambers, “RCS Reduction of Spiral Patch Antenna Using a PSS Boundary,” *IEEE Proceedings—Radar, Sonar and Navigation*, **152**, 4, August 2005, pp. 248-252.

12. L. Xu, D. Feng, Y. Liu, X. Pan and X. Wang, "A Three-Stage Active Cancellation Method Against Synthetic Aperture Radar," *IEEE Sensors Journal*, **15**, 11, November 2015, pp. 6173-6178.
13. P.-Y. Chen, C. Argyropoulos, and A. Alù, "Broadening the Cloaking Bandwidth With Non-Foster Metasurfaces," *Physics Review Letters*, **111**, 23, December 2013, p. 233001.
14. J. C. Soric, P. Y. Chen, A. Kerkhoff, D. Rainwater, K. Melin, et al., "Demonstration of an Ultralow Profile Cloak for Scattering Suppression of a Finite-Length Rod in Free Space," *New Journal of Physics*, **15**, 3, March 2013, p. 033037.
15. M.-J. Haji-Ahmadi, V. Nayyeri, M. Soleimani, and O. M. Ramahi, "Pixelated Checkerboard Metasurface for Ultra-Wideband Radar Cross Section Reduction," *Scientific Reports*, **7**, September 2017, p. 11437.
16. H. B. Baskey, E. Johari, and M. J. Akhtar, "Metamaterial Structure Integrated With a Dielectric Absorber for Wideband Reduction of Antennas Radar Cross Section," *IEEE Transactions on Electromagnetic Compatibility*, **59**, 4, August 2017, pp. 1060-1069.
17. S. Sengupta, H. Council, D. R. Jackson, and D. Onofrei, "Active Radar Cross Section Reduction of an Object Using Microstrip Antennas," *Radio Science*, **55**, 2, February 2020, 1-20.
18. S. Sengupta, H. Council, D. R. Jackson, D. Onofrei, and V. Vellanki, "Active Scattering Cancellation Using a Microstrip Antenna Element," XXXIVth General Assembly and Scientific Symposium of the International Union of Radio Science (URSI GASS), Rome, Italy, Sept. 2021.
19. V. Vellanki, *Radar Cross Section of an Arbitrary Object Using Active Antenna Elements*, Ph.D. dissertation, University of Houston, TX, USA, 2021.
20. D. R. Jackson, "Microstrip Antennas," in J. L. Volakis (ed.), *Antenna Engineering Handbook*, 5th Ed., New York, NY, McGraw Hill Professional, 2018, Chapter 7.